CEAS-GNC-2024-100

EuroGNC Navigation Guidance Control CEAS Bristol, UK June 11th-13th 2024
University of BRISTOL ROYAL AERONAUTICAL SOCIETY AIAA

# Development of the Dynamics, Kinematics, and Environment (DKE) Models for L3GWO

**Andrei F. Cojocaru** GNC/AOCS Engineer, Deimos Space SRL, GNC/AOCS Competence Center, Avionics Business Unit, 011013, Bucharest, Romania. andrei.cojocaru@deimos-space.com

**Alexandru Lapusneanu** GNC/AOCS Engineer, Deimos Space SRL, GNC/AOCS Competence Center, Avionics Business Unit, 011013, Bucharest, Romania. alexandru.lapusneanu@deimos-space.com

**Paulo Rosa** Head of the Avionics Business Unit, Deimos Engenharia Lda, 1070-061 Lisboa, Lisbon, Portugal. paulo.rosa@deimos.com.pt

**Raúl Sánchez Maestro** GNC/AOCS Senior Engineer, SENER Aeroespacial y Defensa, Flight Systems and Avionics Division, C/Severo Ochoa 4, 28760 Tres Cantos, Madrid, Spain, raul.sanchez@aeroespacial.sener

**Jorge Cardin** GNC/AOCS Engineer, SENER Aeroespacial y Defensa, Flight Systems and Avionics Division, C/Severo Ochoa 4, 28760 Tres Cantos, Madrid, Spain, jorge.cardin@aeroespacial.sener

**Joost Veenman** Control expert and project manager, SENER Aeroespacial y Defensa, Flight Systems and Avionics Division, C/Severo Ochoa 4, 28760 Tres Cantos, Madrid, Spain, joost.veenman@aeroespacial.sener

**Valentin Preda** GNC Systems Engineer, European Space Agency, ESTEC, The Netherlands, valentin.preda@esa.int

**Jonathan Grzymisch** GNC Systems Engineer, European Space Agency, ESTEC, The Netherlands, Jonathan.Grzymisch@esa.int

*ABSTRACT*

**This paper describes the Dynamics, Kinematics, and Environment (DKE) modeling approach devised for the DFACS-L3GWO study for Phase A/B1 of the LISA mission. By measuring the very small displacement of the so-called test masses within 3 spacecraft, separated by 2.5 million km, in a rotating triangular formation, 50 million km from the Earth, this mission is set to be the first gravitational wave observatory in space. One of the major challenges in modeling such physics is the uniquely large difference, in orders of magnitude, of the states whose time-evolution is to be described. The formulation proposed addresses specifically this issue, while also considering a wide range of disturbances, including the influence of bodies in the solar system in the overall stability of the satellites formation. The work described herein paved the way for the design and verification of the GNC subsystem, also developed within the DFACS-L3GWO study.**

**Keywords:** dynamics, modeling and simulation, GNC, LISA

# 1 Introduction

The Laser Interferometer Space Antenna (LISA) mission is a large-class mission from ESA, aiming to be the first gravitational wave observatory in space. This goal is to be achieved by placing 3 satellites, separated by 2.5 million km, in a rotating triangular formation, 50 million km separated from the Earth in a Heliocentric Earth Trailing Orbit (HETO) orbit. Each of these satellites is equipped with highly sensitive laser- and interferometry-based sensors, that measure tiny perturbations to the triangle formation, caused by the low-frequency gravitational waves. It is the size of this partially-virtual space structure that makes it possible to sense gravitational waves, i.e., to observe the distortion of the spacetime fabric. Given the accuracy requirements it entails, it comes at the cost of an extremely challenging Guidance, Navigation, and Control (GNC) problem [10].

A key step of the GNC design and validation process typically used in space applications is the modeling of the dynamics of the plant to be controlled. While data-driven approaches to GNC development are available and have been increasingly adopted by the scientific and industrial communities [11], model-based methods tend to be preferred for space missions due to several reasons, such as the typically higher performances and the means to quantify robustness, both to known unknowns (e.g., uncertain mass of the spacecraft), as well as unknown unknowns (dynamics that were not explicitly accounted for in the modeling). Moreover, given the well-known characterization of the disturbances in the space environment, and the thorough knowledge available on the characteristics of sensors and actuators used for space applications, very high-accuracy models can often be obtained.

However, LISA poses significant challenges in terms of modeling, the main one being the several orders of magnitude between the positions of the spacecraft and the small displacements of the test masses inside each of them, which are used to sense the perturbations caused by the gravitational waves. Moreover, equipment such as the telescopes and the High Gain Antenna (HGA) generate multibody dynamics with a significant impact on the overall behavior of the spacecraft.

As such, ESA issued an invitation to tender for the GNC development for LISA [10], with the consortium led by SENER and participated by DEIMOS being one of the selected teams for this activity. Within this project, entitled DFACS-L3GWO, one of DEIMOS' responsibilities was the DKE modeling, which is the topic of the present paper. A key contribution described herein is the formulation of the dynamics problem in such a way that the numerical propagation of the state entails an accuracy level compatible with the stringent requirements of the mission.

The following three dynamics and kinematics configurations for the formation spacecraft (S/C) were considered during the project, allowing for different levels of complexity of the overall DKE. These configurations combine position and attitude propagation (6DOF) of the different S/C and simplified predefined trajectories (3DOF), useful for the different phases of the GNC design and validation:

1. Full formation operative: 3 x 6 DOF (degrees-of-freedom) dynamics propagation.
2. Single S/C testing scenario:
    a. 1 x 6DOF dynamics propagated;
    b. 2 x 3DOF dynamics (i.e., position) tabulated.
3. 3DOF scenarios only.

For each of the scenarios listed above, four S/C configurations (indexed by "k") were considered, representing different phases of the mission:

1. Both Test Masses (TMs) grabbed: +0DOF dynamics propagation (single rigid body).
2. TM1 grabbed and TM2 released: +6DOF dynamics propagation (two rigid bodies).
3. TM1 released and TM2 grabbed: +6DOF dynamics propagation (two rigid bodies).

4. Both TM released (nominal configuration): +12DOF dynamics propagation (three rigid bodies).

The dynamics impacting the S/C and the test masses are described in the following sections, although, due to page limits, some modeling elements are omitted. The remainder of this paper is organized as follows: Sections 2 and 3 describe, respectively, the S/C translational and rotational dynamics; the multi-body dynamics formulation, used for the telescopes and high gain antenna dynamics modeling, when connected to the S/C, is provided in Section 4; the test masses dynamics models are derived in Section 5; Section 6 is devoted to the modeling of disturbances affecting the overall plant; finally, the conclusions are summarized in Section 8.

## 1.1 Notation and Abbreviations

Vectors and matrices are denoted by bold, italic lowercase, $\boldsymbol{a}$, and upper case letters, $\boldsymbol{A}$, respectively. Rotation matrices are denoted by $\boldsymbol{R} \in \mathrm{SO}(3)$ and the external product is denoted by $\times$. The time derivative of vector $\boldsymbol{x}$ is denoted by $\dot{\boldsymbol{x}}$. Each subsection will start with the definition of the variables of interest.

The following abbreviations are used throughout the text:

- CoM: Center-of-Mass
- DKE: Dynamics, Kinematics, and Environment
- DoF: Degrees-of-Freedom
- GRS: Gravity Reference Sensor
- HETO: Heliocentric Earth Trailing Orbit
- HGA: High Gain Antenna
- S/C: SpaceCraft
- SRP: Sun Radiation Pressure
- TM: Test Mass

# 2 Spacecraft Translational Dynamics

The translational dynamics of each spacecraft are formulated in Orbital Inertial Frame [OIF] (cf. Annex I):

$$\ddot{\boldsymbol{R}}_{SC} = \boldsymbol{a}_g + \frac{1}{m_{SC,k}}(\boldsymbol{f}_t + \boldsymbol{f}_d) \qquad \text{Eq. 2-1}$$

with:

- $\ddot{\boldsymbol{R}}_{SC}$: S/C CoM translational absolute acceleration in [OIF].
- $m_{SC,k}$: S/C mass of configuration "k".
- $\boldsymbol{a}_g$: gravitational acceleration.
- $f_t$: reaction control system force (DKE input).
- $f_d$: disturbing force.

The gravitational acceleration acting on $S/C_i$ is the solution of the restricted N-body problem (RNBP), written as follows:

$$\boldsymbol{a}_g = -\sum_j \frac{\mu_j}{\left|\boldsymbol{R}_j\right|^3}\boldsymbol{R}_j \qquad \text{Eq. 2-2}$$

with:

- $\mu_j$: gravitational constant of the celestial body *'j'*.

- $\boldsymbol{R}_j$: relative position of the celestial body *'j'* with respect to the S/C.

The spacecraft absolute velocity $\dot{\boldsymbol{R}}_{SC}$ and position $\boldsymbol{R}_{SC}$ are then obtained from direct integration (dynamics propagation) starting from the initial conditions (Subsection 2.1).

The modelled disturbing force $\boldsymbol{f}_d$ acting on the S/C is composed of:

$$\boldsymbol{f}_d = \boldsymbol{f}_{d,int} + \boldsymbol{f}_{srp} + \boldsymbol{f}_{met} \qquad \text{Eq. 2-3}$$

being:

- $\boldsymbol{f}_{d,int}$: internal disturbing force.
- $\boldsymbol{f}_{srp}$: solar radiation pressure.
- $\boldsymbol{f}_{met}$: micro-meteoroids impact.

## 2.1 LISA Orbits

The three LISA S/C are placed at the vertices of an equilateral triangle with a side length of $l = 2.5 \cdot 10^6\ km$. The formation is bound to a *cartwheel orbit*, where the S/C (*slave*) is following an apparent circular motion about a *master* while orbiting the Sun, on a plane tilted by $\phi = 60º$ with respect to the Ecliptic. The formation is on a HETO, i.e., on the Earth orbit, at an angular distance $\gamma \sim 20^o$ from the Earth.

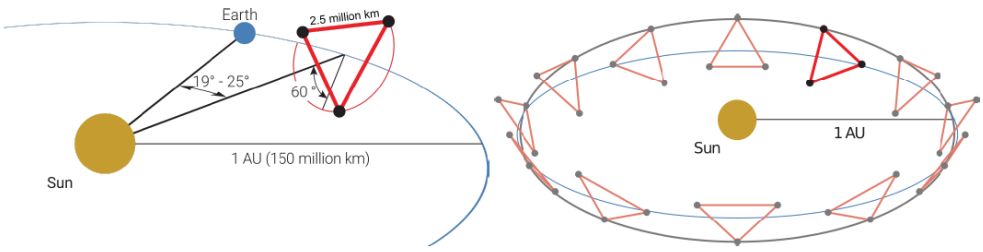


**Figure 2-1: LISA cartwheel orbit (taken from the Design Description LISA Payload document, ESA-L3-EST-INST-DD-001)**

The c*artwheel orbit* is a solution to the *Clohessy-Whiltshire* equations in the master satellite *Hill's reference frame*. The slave satellite orbits the master on a circular orbit with a period equal to the orbital period of the master. For the specific case of LISA, the master is on a circular orbit around the Sun, with an orbital radius equal to the semi-major axis of the Earth orbit ($a$). The two S/C are then symmetrically dispersed with respect to the initial Hill's reference frame of the formation's *master*.

The Hill's frame defined orbits are then rotated in the Orbital Inertial frame [OIF] (Annex I) according to the inertial position of the Earth ($\boldsymbol{R}_{E,0}$) and then translated considering the inertial position and velocity of the Sun ($\boldsymbol{R}_{S,0}, \dot{\boldsymbol{R}}_{S,0}$) with respect to the Solar System Barycenter (SSB) at the initial epoch (parameter). The resulting nominal orbits of the LISA formation S/C are depicted in Figure 2-2 (where the formation *arm-length* is augmented 10 times to better illustrate the formation evolution).

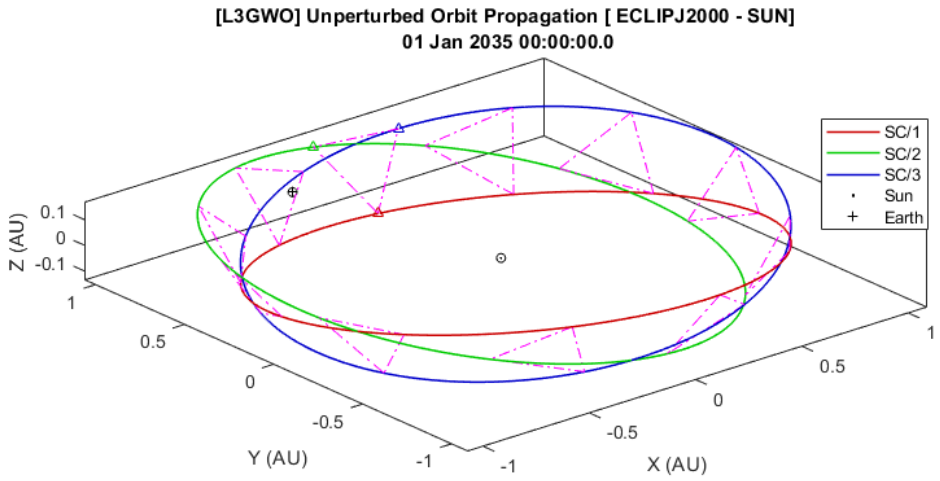


**Figure 2-2: Analytical orbits evolution in Orbital Inertial frame [OIF], centered in the Sun. Formation arm-length is off-scaled (10x magnified) to highlight the formation evolution at 1AU. Initial positions (S/C and Earth) at UTC0.**

## 2.2 Cowell's Propagation Results (R-2BP)

As a preliminary step, the LISA S/C initial state at UTC0 has been propagated considering the only Newtonian gravitational acceleration of the Sun in Eq. 2-2 (**R-2BP**). The impact of other bodies is addressed in Section 6.2. The following figures illustrate the fact that the LISA requirements (dashed red lines), for a 10-year propagation, are satisfied with no need for formation maintenance maneuvering, in this ideal scenario that assumes no impact from disturbances, and neglecting propagation errors, which were deemed sufficiently small when compared to the analytical solution.

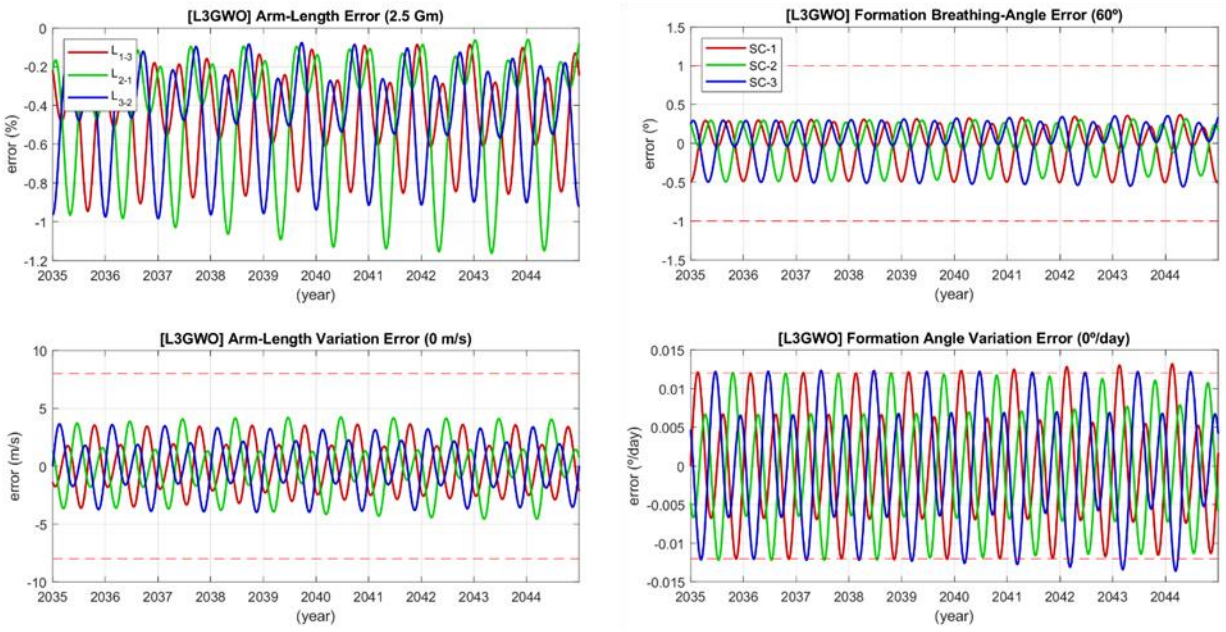


**Figure 2-3: R2BP - evolution of the formation arm-length/velocity error (left) and breathing angle/angular velocity error (right). Requirements thresholds are red-dashed.**

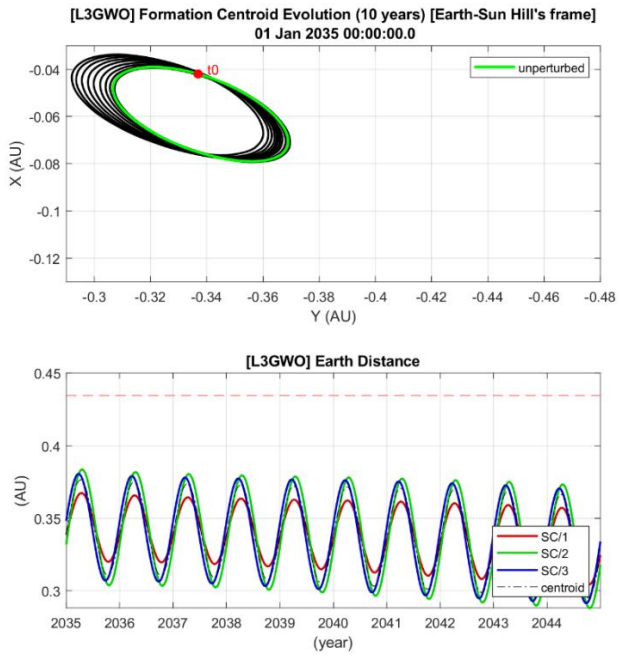


**Figure 2-4: R2BP - evolution of the formation centroid (top) in the Earth-Sun Hill's frame [EHF] and of the S/C distance from the Earth. Requirement threshold is red-dashed.**

# 3 Spacecraft Rotational Dynamics

Each S/C angular dynamics is formulated in an absolute way from the inertial frame [OIF] to the S/C Rigid Body Frame [RBF] (Annex I), expressed in [RBF], according to the rigid body Euler dynamics:

$$\boldsymbol{h}_{SC} = \boldsymbol{I}_{SC,k}\,\boldsymbol{\omega}_{SC} \qquad \text{Eq. 3-4}$$

with:

- $\boldsymbol{\omega}_{SC}$: S/C angular velocity with respect to the inertial frame, in [RBF].
- $\boldsymbol{I}_{SC,k}$: S/C inertia tensor (configuration "k") in [RBF].

The total derivative of the S/C angular momentum is then:

$$\boldsymbol{I}_{SC,k}\,\dot{\boldsymbol{\omega}}_{SC} + \dot{\boldsymbol{I}}_{SC,k}\boldsymbol{\omega}_{SC} + \boldsymbol{\omega}_{SC} \times \left(\boldsymbol{I}_{SC,k}\,\boldsymbol{\omega}_{SC}\right) = \boldsymbol{l}_t + \boldsymbol{l}_d \qquad \text{Eq. 3-5}$$

given:

- $\boldsymbol{l}_t$: reaction control system torque acting on the S/C, in S/C body frame (DKE input).
- $\boldsymbol{l}_d$: disturbing torque acting on the S/C, in S/C body frame.

Thus, one can write the S/C angular velocity final equation in the S/C body frame as:

$$\dot{\boldsymbol{\omega}}_{SC} = \boldsymbol{I}_{SC,k}^{-1}\left(\boldsymbol{l}_t - \dot{\boldsymbol{I}}_{SC,k}\boldsymbol{\omega}_{SC} - \boldsymbol{\omega}_{SC} \times \left(\boldsymbol{I}_{SC,k}\,\boldsymbol{\omega}_{SC}\right) + \boldsymbol{l}_d\right) \qquad \text{Eq. 3-6}$$

The modeled disturbing torque $\boldsymbol{l}_d$ acting on the S/C is composed of the following terms:

$$\boldsymbol{l}_d = \boldsymbol{l}_{d,R} + \boldsymbol{l}_{d,int} + \boldsymbol{l}_{srp} + \boldsymbol{l}_{GG} + \boldsymbol{l}_{met} \qquad \text{Eq. 3-7}$$

with:

- $\boldsymbol{l}_{d,R}$: rotating systems disturbing torque.
- $\boldsymbol{l}_{d,int}$: internal disturbing torque.
- $\boldsymbol{l}_{srp}$: solar radiation pressure.
- $\boldsymbol{l}_{GG}$: gravity gradient.
- $\boldsymbol{l}_{met}$: micro-meteoroids impact.

# 4 Spacecraft Multi-Body Dynamics

We consider the diagram in Figure 4-5 to support the formulation of the rotating elements disturbing torque coupling. The Geometric reference frame here introduced is defined in Annex I.

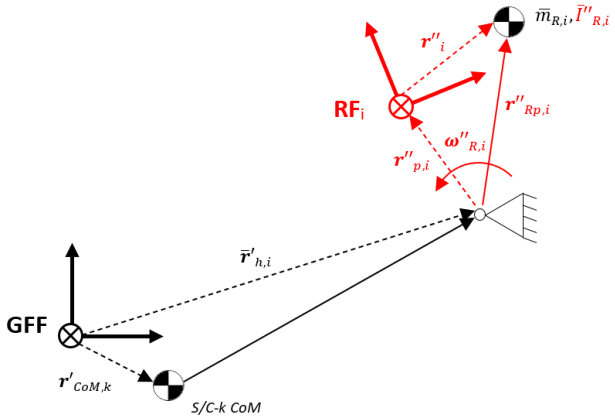


**Figure 4-5: Schematics used to support the derivation of the rotating elements disturbing torque.**

The contribution of the rotating systems, namely the two telescopes and the High-Gain Antenna (HGA), to the pot of the disturbances is here below formulated in terms of resulting **disturbing torque**.

We start from the overall angular momentum balance, updating Eq. 3-4:

$$\boldsymbol{h}_{TOT} = \boldsymbol{h}_{SC} + \sum_i \boldsymbol{h}_{R,i} \qquad \text{Eq. 4-8}$$

with:

- $\boldsymbol{h}_{TOT}$: total angular momentum of the multibody system in [RBF].
- $\boldsymbol{h}_{SC}$: angular momentum of the S/C in [RBF] (Eq. 3-4).
- $\boldsymbol{h}_{R,i}$: angular momentum of the rotating system *'i'* in [RBF].

Deriving Eq. 4-8 in time we get the definition of the disturbing torque of the rotating systems:

$$\frac{d\boldsymbol{h}_{TOT}}{dt} = \frac{d\boldsymbol{h}_{SC}}{dt} + \sum_i \frac{d\boldsymbol{h}_{R,i}}{dt} \qquad \text{Eq. 4-9}$$

$$\frac{d\boldsymbol{h}_{TOT}}{dt} = \dot{\boldsymbol{I}}_{SC}\,\boldsymbol{\omega}_{SC} + \boldsymbol{I}_{SC}\,\dot{\boldsymbol{\omega}}_{SC} + \boldsymbol{\omega}_{SC} \times (\boldsymbol{I}_{SC}\,\boldsymbol{\omega}_{SC}) + \sum_i \frac{d\boldsymbol{h}_{R,i}}{dt} \qquad \text{Eq. 4-10}$$

$$\boldsymbol{l}_{d,R} = -\sum_i \frac{d\boldsymbol{h}_{R,i}}{dt} \qquad \text{Eq. 4-11}$$

The angular momentum of rotating system *'i'* is given by:

$$\begin{aligned}\boldsymbol{h}_{R,i} = \boldsymbol{C}^{\tau}_{S\to Ri}\,\Big(&\bar{\boldsymbol{I}}''_{R,i}\,\boldsymbol{\omega}''_{R,i} + \bar{m}_{R,i}\,\bar{\boldsymbol{r}}''_{Rp,i} \times \big(\boldsymbol{\omega}''_{R,i} \times \bar{\boldsymbol{r}}''_{Rp,i}\big)\Big) \\ &+ \bar{m}_{R,i}\,\big(\bar{\boldsymbol{r}}'_{h,i} - \boldsymbol{r}'_{CoM,k}\big) \times \Big[\boldsymbol{C}^{\tau}_{S\to Ri}\big(\boldsymbol{\omega}''_{R,i} \times \bar{\boldsymbol{r}}''_{Rp,i}\big)\Big]\end{aligned} \qquad \text{Eq. 4-12}$$

with:

- $\boldsymbol{C}_{S\to Ri}$ : rotation matrix from [RBF] to the local rotating frame.
- $\bar{\boldsymbol{I}}''_{R,i}$: inertia tensor of the rotating system *'i'* with respect to its CoM, expressed in the local rotating frame (fixed parameter).
- $\bar{m}_{R,i}$: mass of the rotating system *'i'* (fixed parameter).
- $\boldsymbol{\omega}''_{R,i}$: relative angular velocity of the rotating system *'i'* with respect to [RBF], expressed in the local rotating frame.

- $\bar{\boldsymbol{r}}'_{h,i}$: position of the rotating element pivoting point in [GFF] (fixed parameter).
- $\boldsymbol{r}'_{CoM,k}$: position of the S/C-k CoM in [GFF].
- $\bar{\boldsymbol{r}}''_{Rp,i}$: position of the rotating element CoM with respect to the pivoting point, in the local rotating frame (fixed parameter):

$$\bar{\boldsymbol{r}}''_{Rp,i} = \bar{\boldsymbol{r}}''_{p,i} + \bar{\boldsymbol{r}}''_{i} \qquad \text{Eq. 4-13}$$

The formulation in Eq. 4-12 can be simplified by noting that the first contribution represents the rotating element inertia tensor translated to the pivoting point, and thus the final expression of the rotating element angular momentum is given by:

$$\boldsymbol{h}_{R,i} = \boldsymbol{C}^{\tau}_{S\to Ri}\left(\bar{\boldsymbol{I}}''_{Rp,i}\,\boldsymbol{\omega}''_{R,i}\right) + \bar{m}_{R,i}\left(\bar{\boldsymbol{r}}'_{h,i} - \boldsymbol{r}'_{CoM,k}\right) \times \boldsymbol{C}^{\tau}_{S\to Ri}\left(\boldsymbol{\omega}''_{R,i} \times \bar{\boldsymbol{r}}''_{Rp,i}\right) \qquad \text{Eq. 4-14}$$

with this term being interpreted as a disturbing angular momentum contributing to the angular dynamics.

## 4.1 Telescopes

The strawman concept of the (Gravity Reference Sensor) GRS - Optical bench - telescope assembly on LISA is depicted in Figure 4-6. The telescope and the GRS are rigidly connected. The whole assembly is allowed to rotate about a pivot point in order to satisfy the breath angle $\alpha$ requirements dictated by the evolution of the formation in time. The approach described above was applied to the telescopes to derive their impact on the dynamics, as well as on the inertia of the overall system.

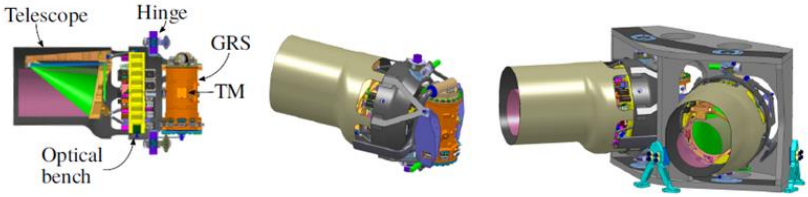


**Figure 4-6: Strawman design of the optical assembly [1]. The optical assembly defined by the telescope, the GRS and the optical bench rotate around a common pivot (hinge).**

## 4.2 High Gain Antenna

For the specific case of the HGA, the rotation matrix from [RBF] to the local rotating frame ($\boldsymbol{C}_{S\to A}$) is defined in terms of two angles: Azimuth ($\alpha_A$) and Elevation ($\beta_A$) from the antenna mounting base frame. A similar approach as for the telescopes has been employed for modeling.

# 5 Test Masses Dynamics

Figure 5-7 depicts the schematics used to support the formulation of the Test Masses linear and rotational dynamics.

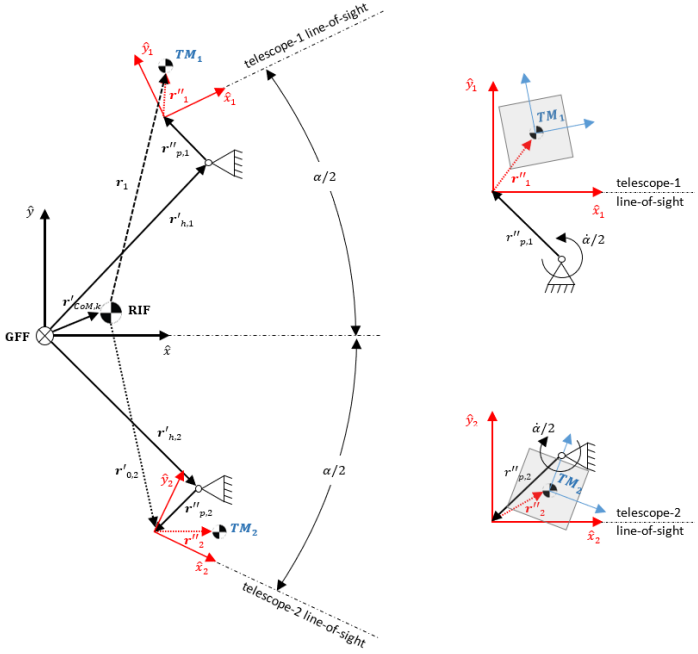


**Figure 5-7: Schematics used to support the derivation of the TM translational and angular dynamics. Depicted S/C body frame and the two Telescope Frames. Highlighted the displacements and the rotational kinematics.**

## 5.1 Translational Dynamics

Treating the TM linear dynamics independently from the S/C, we can write the Newtonian absolute formulation for the TM-i in the Orbital Inertial Frame [OIF] as follows:

$$\ddot{\boldsymbol{R}}_i = \boldsymbol{g}_i + \frac{1}{m_i}\boldsymbol{f}_{d,i} + \frac{1}{m_i}\boldsymbol{f}_i - \frac{\boldsymbol{K}_i}{m_i}\left(\boldsymbol{R}_i - \boldsymbol{R}_{0,i}\right) \qquad \text{Eq. 5-15}$$

with:

- $\boldsymbol{g}_i$: gravitational inertial acceleration (external) in [OIF].
- $\boldsymbol{f}_{d,i}$: disturbing force (internal/external) in [OIF].
- $m_i$: mass of TM-i.
- $\boldsymbol{f}_i$: force exerted by the electrostatic suspension system (internal) in [OIF].
- $\boldsymbol{K}_i$: TM-i electrostatic suspension stiffness matrix in [OIF].
- $\boldsymbol{R}_i$: TM-i CoM inertial position in [OIF].
- $\boldsymbol{R}_{0,i}$: TM-i CoM rest inertial position in [OIF].

However, this absolute formulation is sensitive to the numerical integration errors, due to the propagation of large-scale quantities (e.g., the distance to the Sun), while handling small variations in the TM position with respect to rest (issue less relevant for Earth-centered orbits). This can be more clearly appreciated in Figure 5-8, showing the error divergence in time.

An alternative formulation of the TM linear dynamics propagation relative to the S/C CoM was therefore implemented: we introduced the Relative Inertial Frame [RIF] (Annex I). We define $\boldsymbol{r}_i$ as the relative position of TM-i from the S/C CoM in [RIF]. The TM-i linear dynamics equation becomes:

$$\ddot{\boldsymbol{r}}_i = \ddot{\boldsymbol{R}}_i - \ddot{\boldsymbol{R}}_{SC} \qquad \text{Eq. 5-16}$$

Hence:

$$\ddot{\boldsymbol{r}}_i = \boldsymbol{g}_i + \left(\frac{1}{m_i}\boldsymbol{f}_{d,i} + \frac{1}{m_i}\boldsymbol{f}_i - \frac{\boldsymbol{K}_i}{m_i}\left(\boldsymbol{r}_i - \boldsymbol{C}^{\tau}_{I\to S}\boldsymbol{r'}_{0,i}\right) - \ddot{\boldsymbol{R}}_{SC}\right) \quad \text{Eq. 5-17}$$

The comparison of the precision performance is shown in Figure 5-8, where the Keplerian analytical solution is used as reference. The performance shown through the second formulation is unreachable by Eq. 5-15 even with the finest integration tolerance.

Differently from the more intuitive formulation in GRS-i frame, with this formulation there are no transport terms related to the rotational dynamics of the telescope-i frame (i.e., S/C angular velocity + telescope-i frame rotation rate with respect to the S/C), thus minimizing the computational noise error to be integrated. It is stressed that this is a key result of this paper, since this formulation effectively enables the modeling of the dynamics of the spacecraft and the test masses within the same framework, with an accuracy that is well-within the requirements of the mission.

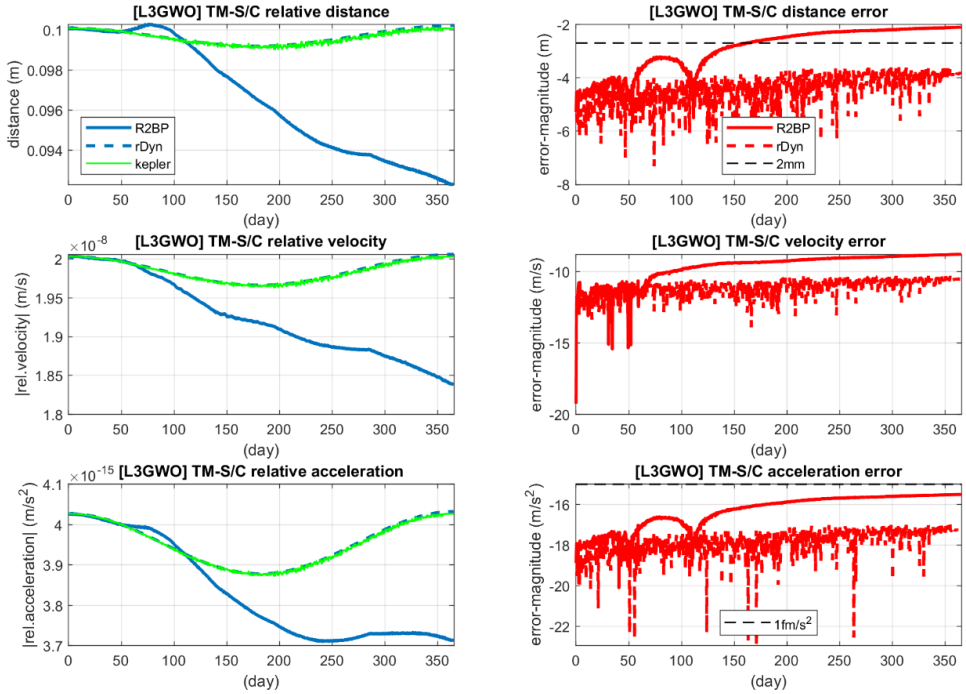


**Figure 5-8: Precision comparison in terms of relative-distance, relative-velocity and relative-acceleration of the TM with respect to the S/C CoM, between Absolute Inertial Orbital-Dynamics propagation (solid-blue) and Inertial Relative-Dynamics Propagation (dashed-blue) vs. the Keplerian analytical solution (green). Thresholds (black-dashed) on position and accelerations are displayed.**

The relative state of TM-i with respect to its GRS-i frame is then retrieved a-posteriori, i.e., after the decoupled integration of the translational dynamics and the rotational one.

## 5.2 Rotational Dynamics

The angular dynamics of the TM-i are formulated considering the Euler rigid body formulation, propagating the TM-i attitude dynamics with respect to [OIF], in local TM-i frame (Annex I):

$$\dot{\boldsymbol{\omega}}_{TM,i} = \boldsymbol{I}_i^{-1}\left(\boldsymbol{l}_i + \boldsymbol{l}_{d,i} - \boldsymbol{\omega}_{TM,i} \times \left(\boldsymbol{I}_i\boldsymbol{\omega}_{TM,i}\right) - \boldsymbol{K}_{\phi,i}\left(\boldsymbol{\phi}_i - \boldsymbol{\phi}_{0,i}\right)\right) \quad \text{Eq. 5-18}$$

with:

- $\dot{\boldsymbol{\omega}}_{TM,i}$: absolute TM-i angular acceleration in TM-i frame.
- $\boldsymbol{I}_i$: TM-i inertia tensor with respect to TM-i CoM, in TM-i frame.
- $\boldsymbol{l}_i$: torque exerted by the electrostatic suspension system (internal), in TM-i frame.

- $\boldsymbol{l}_{d,i}$: disturbing torque (internal/external), in TM-i frame.
- $\boldsymbol{K}_{\phi,i}$: TM-i electrostatic suspension torsional stiffness matrix, in TM-i frame.
- $\boldsymbol{\phi}_i$: TM-i absolute attitude.
- $\boldsymbol{\phi}_{0,i}$: TM-i absolute rest attitude.

## 5.3 Internal Forces and Torques

The internal forces and torques were taken into account to compute the equivalent internal disturbing force and torque acting on the S/C, in order to preserve the total linear and angular momentum of the system (S/C+TM). Considering the variation of the linear momentum (in the inertial frame) due to internal forces, the overall system balance leads to:

$$\Delta \boldsymbol{p}_{d,int} = -\Delta \boldsymbol{p}_{i,int} \qquad \text{Eq. 5-19}$$

naming $\Delta \boldsymbol{p}_{d,int}$ and $\Delta \boldsymbol{p}_{i,int}$ the variation of the linear momentum respectively of the S/C and the TM-i.

Differentiating it in time, the internal disturbing force acting on the S/C CoM is equivalent to:

$$\boldsymbol{f}_{d,int} = -\boldsymbol{f}_{i,int} \qquad \text{Eq. 5-20}$$

being $\boldsymbol{f}_{i,int}$ the resultant of the internal forces between the S/C and TM-i, acting on TM-i (Eq. 5-17):

$$\boldsymbol{f}_{i,int} = \boldsymbol{f}_i + \boldsymbol{f}_{d,i} - \boldsymbol{K}_i(\boldsymbol{r}_i - \boldsymbol{r}_{0,i}) \qquad \text{Eq. 5-21}$$

$\boldsymbol{f}_{d,i}$ entails **internal** forces contribution such as self-gravity disturbances.

Analogously, considering the variation of the angular momentum in [RBF] and differentiating it in time, the internal disturbing torque acting on the S/C is:

$$\boldsymbol{l}_{d,int} = -\left(\boldsymbol{C}^{\tau}_{S\to i}\boldsymbol{l}_{i,int} + \boldsymbol{C}_{I\to S}(\boldsymbol{r}_i \times \boldsymbol{f}_{i,int})\right) \qquad \text{Eq. 5-22}$$

being:

- $\boldsymbol{r}_i$: relative position of TM-i in [RIF] (Eq. 5-17).
- $\boldsymbol{f}_{i,int}$: internal force in [RIF] (Eq. 5-21).
- $\boldsymbol{l}_{i,int}$: resultant of the internal torques between the S/C and the TM-i, acting on TM-i.

$$\boldsymbol{l}_{i,int} = \boldsymbol{l}_i + \boldsymbol{l}_{d,i} - \boldsymbol{K}_{\phi,i}(\boldsymbol{\phi}_i - \boldsymbol{\phi}_{0,i}) \qquad \text{Eq. 5-23}$$

# 6 Disturbances Modeling

The disturbances acting upon the S/C play a major role in the evolution of the formation, with a non-negligible impact on the behavior of each S/C in the frequency ranges of scientific interest for the mission. Hence, a thorough modeling and validation of a wide range of disturbances was performed within the DFACS-L3GWO project, with some highlights described in the sequel.

## 6.1 Sun Gravity Field

The gravity field of the Sun was assumed uniform in space (i.e., without mass-distribution dependent gravity harmonics). Hence, no disturbing linear accelerations depending on the solar gravity field were considered.

Gravity-Gradient Torque

The variation of the solar gravity field with the square of the distance is responsible for affecting the rotational dynamics of non-uniform mass distributed spacecraft. The gravity-gradient is hence modelled

for each S/C at least, while under the assumption of perfect uniform cubic TMs these are not affected by such a disturbance. The gravity-gradient torque arising is orthogonal to the S/C position and inversely proportional to the cube of the solar distance. Its general formulation is provided in [6].

## 6.2 Gravitational disturbances of celestial bodies

The celestial bodies of the Solar System have an influence on both the S/C and TM acceleration. This disturbing acceleration can be computed through Eq. 2-2. Figure 6-1 depicts the comparison between the acceleration magnitudes of the main body (Sun) and the sum of the 8 Solar System celestial bodies. While the influence of the Sun is several orders of magnitude stronger than that of the remaining celestial bodies, the impact of the latter, in the long term, is not negligible, as described next.

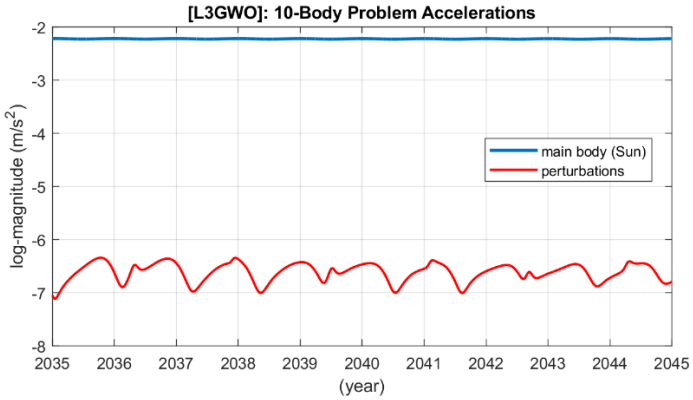


**Figure 6-1: Main body perturbation (blue), third-bodies total perturbation (red). 10y evolution starting on Jan the 1st 2035 at 00:00 UTC.**

By incrementally adding the number of celestial bodies in the translational dynamics propagation (RNBP), it was concluded that for N>4 (i.e., starting considering the Earth-Moon system perturbation), the formation geometry drifts outside the requirements boundaries after 5 years (with no orbit control). Moreover, due to the "pulling" action of the Earth-Moon system, this system is feeding energy to the formation orbits, which is translated into a semi-major axis increasing, together with the orbital period, which explains the divergence of the constellation from the Earth (Figure 6-2), exceeding the maximum allowed distance after 7 years of propagation (even without considering the control forces performed by the GNC during the drag-free phases).

Analyzing the approximation error in considering a reduced number of bodies (N>3) if compared to the highest detailed model (N=11), it was concluded that N=7 is enough for the celestial bodies perturbing acceleration description (in terms of impact on the formation evolution). The 5 planets considered for N=7 were: Jupiter, Earth, Venus, Saturn, and Mars.

The DKE was therefore implemented as being parameterizable, allowing for the selection of the number of celestial bodies to be considered, having as guideline: N=2, if it is desired to focus on the pure DFACS, considering the formation to be externally maintained; N>4 (Jupiter and Earth at least), if active formation maintenance is foreseen.

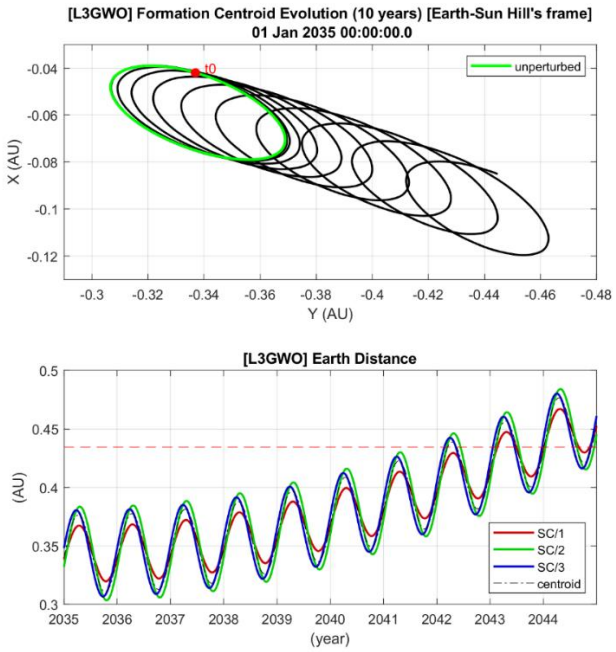


**Figure 6-2: R7BP - evolution of the formation centroid (top) in the Earth-Sun Hill's frame and of the S/C distance from the Earth, considering the restricted 3-body problem. Requirement threshold is red-dashed.**

## 6.3 Self-Gravity

Self-gravity is meant to affect internally both the TM-i dynamics and the S/C. It contributes differently in two ways:

- As a secular component, translated into a DC contribution.
- As gradient contribution, mechanically modelled as a stiffness at GRS.

As described in [3], [4] and [5], the S/C self-gravity gradient, together with the electrostatic/magnetic interactions, create a virtual spring-mass system, which has been considered through the stiffness matrix in the TM-i translational and rotational dynamics. Their contribution (translational/rotational) are reflected in the S/C dynamics to preserve the total linear/angular momentum.

## 6.4 Solar Radiation Pressure

The Solar Radiation Pressure (SRP) is the most prominent environmental non-gravitational disturbance acting on the LISA S/C [7], affecting only the S/C and not the TMs. As per [9], the SRP fluctuation is modelled as a colored noise with a power law of $f^{-1/3}$ and a Gaussian distribution.

Due to the distance of the LISA formation from the Earth (~60E6 km) and the nature of the orbit (HETO), all the radiation disturbances coming from the Earth that are usually considered in Earth-centered orbits are here discarded. These are: Earth and Moon eclipse, Earth albedo and Earth IR radiation [6].

The magnitude of the solar direct radiation flux Φ received by the S/C results from the modulation of the mean solar flux at 1AU ($\Phi_0$) by the variability of the distance between the Sun and the S/C. The flux direction $\boldsymbol{u}$ [OIF] is determined by the Sun-spacecraft vector direction.

$$\boldsymbol{\Phi} = \Phi_0 \frac{|\boldsymbol{R}_0|^2}{|(\boldsymbol{R}_{SC} - \boldsymbol{R}_{SUN})|^2} \boldsymbol{u} \qquad \text{Eq. 6-24}$$

$$\boldsymbol{u} = \frac{\boldsymbol{R}_{SC} - \boldsymbol{R}_{SUN}}{|\boldsymbol{R}_{SC} - \boldsymbol{R}_{SUN}|} \quad \text{Eq. 6-25}$$

SRP Force

The SRP perturbing force appears in satellite surfaces exposed to the direct solar radiation flux. The computation of this force is formulated based on the geometric and physical parameters of the spacecraft as defined by the geometric layout model, which features the S/C as an assembly of flat plates. More specifically, the overall SRP force acting on the satellite center of mass is given by Eq. 6-26, where $\boldsymbol{\Phi}$ denotes the radiation flux (Eq. 6-24), which is assumed parallel for all the surfaces, $c$ is the speed of light, $A_i$ represents the area of the i-th panel and $\boldsymbol{c_i}$ is the coefficients vector.

$$\boldsymbol{f}_{srp} = \sum_i \boldsymbol{f}_{srp,i} \quad \text{Eq. 6-26}$$

$$\boldsymbol{f}_{srp,i} = \frac{|\boldsymbol{\Phi}|}{c} A_i \boldsymbol{c_i} \quad \text{Eq. 6-27}$$

The SRP coefficients $\boldsymbol{c_i}$ depend on the direction of the solar radiation $\boldsymbol{u}$ (Eq. 6-25), the normal surface vector $\boldsymbol{n}_i$ and the absorption, specular reflection and diffuse reflection factors $k_{a,i}$, $k_{s,i}$ and $k_{d,i}$ respectively. A preliminary estimation of the SRP acceleration magnitude for a LISA-like S/C at 1AU is provided in [8] and it is in the order of $4 \cdot 10^{-8} m/s^2$.

SRP Torque

Each S/C panels' properties contain, within the geometric specifications, the position of the panels' center of pressure $\boldsymbol{r'}_{c,i}$ with respect to the S/C CoM. Due to this offset, the SRP force acting on panel *'i'* also generates a disturbing torque.

Solar Flux Variation Model

As described in [9], the variation of the solar constant at 1AU is $\delta\Phi/\Phi = 0.13\%\ Hz^{-1/2}$ at 1mHz, with a $(1/f)^{1/3}$ dependence. Considering the formulation of the SRP acceleration noise provided in [9], the PSD of the solar constant Φ is given by:

$$S_{\Phi\_srp} \approx \left[0.0026 \cdot \Phi \cdot (\,1mHz\,/\,f\,)^{1/3}\right]^2 \quad [(W/m^2)^2/Hz] \quad \text{Eq. 6-28}$$

## 6.5 Magnetic Disturbances

As described in [3], [4] and [5], the internal electrostatic/magnetic coupling between the S/C and the TM is modeled together with the self-gravity as a virtual spring-mass system, address in DFACS-L3GWO through the stiffness matrix in the TM-i translational and rotational dynamics (Annex I). Their contribution (translational/rotational) are reflected in the S/C dynamics to preserve the total linear/angular momentum (Section 5.3).

Physical Model

Differential external magnetic disturbances in LISA (S/C and TM) result from the interaction between any residual magnetic field on board (S/C and TM-i, differently) and the external magnetic field.

The instantaneous magnetic disturbance torque $\boldsymbol{l}_{mag}$ (Nm) due to the external magnetic flux density $\boldsymbol{B}$ (Wb/m$^2$) acts differently on the S/C and the TM according to each residual magnetic moment $\boldsymbol{m}_i$ (Am$^2$):

$$\boldsymbol{l}_{mag} = \boldsymbol{m}_i \times \boldsymbol{B} \quad \text{Eq. 6-29}$$

The instantaneous magnetic disturbance force $\boldsymbol{f}_{mag}$ (N) is computed as:

$$\boldsymbol{f}_{mag} = (\boldsymbol{m}_i \cdot \boldsymbol{\nabla})\boldsymbol{B} \quad \text{Eq. 6-30}$$

where $\boldsymbol{f}_{mag}$ is the Lorentz force acting on the charged system (S/C or TM), as it moves through $\boldsymbol{B}$.

The external magnetic field accounted for LISA is the interplanetary magnetic field (IMF), which is a weak field, varying in strength near the Earth from 1 to 37 nT, with an average value of ~6 nT.

The individual residual magnetic moment is caused by permanent and induced magnetism and the internally generated current loops [6]. The magnitude of the coupling with the IMF depends on the S/C and TM dipoles magnitude ($Am^2$).

Due to the distance of the LISA formation from the Earth (~60e6 km) and the nature of the orbit (HETO), no coupling with the Earth magnetic field is considered, nor is it with the Earth magnetotail (the latter along the Sun-Earth direction).

The disturbance torque coming from the induced *Eddy currents* and magnetic *hysteresis* are here modelled as well. This torque acts on the S/C as well as the TM and it is related to the spinning motion ($\boldsymbol{\omega}_i$) of the body (LISA case) within the external magnetic field. The effect is the precession of the spin axis and a decay of the spinning:

$$\boldsymbol{l}_{Eddy} = k_{e,i}(\boldsymbol{\omega}_i \times \boldsymbol{B}) \times \boldsymbol{B} \quad \text{Eq. 6-31}$$

given $k_{e,i}$ the *Eddy* constant of the body (S/C and TM) depending on its geometry and conductivity.

Allocated Acceleration

Due to the uncertainty on the quantities required to retrieve the external magnetic disturbances coupling, the approach adopted was to disperse the differential magnetic acceleration allocation acting on the TMs only. The total allocated acceleration PSD of the magnetic disturbance variation is given by:

$$S_{acc\_mag} = \left[4\ fm/s^2/\sqrt{Hz}\right]^2 (\ 0.1\ mHz\ /\ f\ )^2 + \left[0.5\ fm/s^2/\sqrt{Hz}\right]^2 \quad \text{Eq. 6-32}$$

The analysis performed have shown that the resulting amplitude spectral density at the minimum frequency of interest ($20\mu Hz$) is still below the threshold of the disturbances to be compensated.

## 6.6 Micrometeoroids Impacts

Micrometeoroids impacts are intended to perturb the linear and the angular dynamics of the **S/C only**, hence not affecting the TMs. The approach adopted in this project was to model the micrometeoroids impacts as linear momentum transfer of a compound Poisson distribution collision probability [1]. This was furthermore consolidated in LPF micro-meteoroid events analysis [2]. The modeling and results obtained are omitted in this paper due to its page limitations.

# 7 Validation approach

An extensive validation campaign was performed within DFACS-L3GWO, devising specific tests for each feature. The validation of the models consists of defining a sequence of applied forces and torques that are defined in inertial space. They are then transformed into the correct frame in accordance to the simulated S/C, Telescope and TM attitudes before injecting them into the equations. Since the force and torque inputs are specified in inertial frame, it is straightforward to determine the corresponding linear and angular momentum of the system when evaluated in inertial frame. Moreover, the results were

compared against those obtained with the dynamics models developed by SENER [10], which were developed independently but whose parameterization was tailored to control design purposes.

In the LISA mission, the dynamic variations can be extremely small. In order to distinguish numerical errors from implementation errors, the mass property values of all individual elements, telescope motion and initial S/C rate are highly exaggerated. (The numerical values therefore do not represent the real LISA mission, but are deliberately chosen for validation purposes). For the same reason all the internal geometric symmetries have been removed.

As an example, we consider a test in which no external actions are performed, but internal forces are applied to the TMs. Due to the absence of external actions, it is expected that the internal forces and torques acting on the two TMs affect consistently the S/C linear and angular momentum, such that the overall system linear and angular momenta in the inertial frame is constant (null). This is apparent in the results illustrated in Figure 7-3.

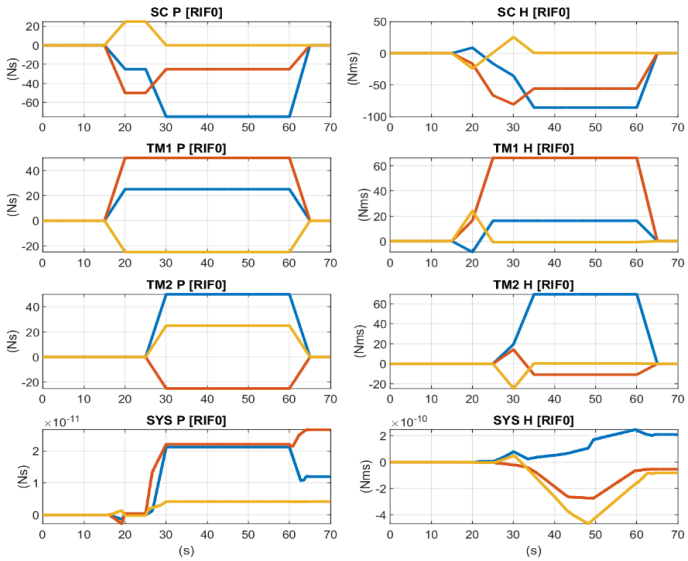


**Figure 7-3: Example of a model validation test – linear momentum (P) and angular momentum (H) of SC, TMs and the overall system (SYS)**

# 8 Conclusions

This paper provided an overview of the DKE modeling approach devised for the DFACS-L3GWO study for Phase A/B1 of the LISA mission, focusing on the key challenges stemming from the several orders of magnitude of difference between signals. A particular effort has also been put on the modeling of the wide range of disturbances that can impact on the dynamics of the S/C and the test masses, at a multitude of frequencies, and with different orders of magnitude. It was also shown that active formation maintenance is required, due to the influence of the closest bodies in the solar system.

The models herein derived were a key element to the proper design and verification of the GNC subsystem, developed in the remainder of the DFACS-L3GWO study, and can serve as the basis for future similar studies and missions.

# Acknowledgments

This work was performed within the DFACS-L3GWO [10] activity led by SENER Aeroespacial y Defensa, Spain, in collaboration with DEIMOS Engenharia, Portugal, and funded by the European Space Agency (ESA), contract no. 4000129130/19/NL/CRS.

The authors acknowledge the key contributions to this work provided by the former project team member Mr. Samuele Salvi.

# References

[1] Sagnieres L.B.M., Sharf I., (2017). Stochastic modelling of hypervelocity impacts in attitude propagation of space debris, Adv. Space Res., 59, 1128-1143, DOI: 10.1016/j.asr.2016.11.030

[2] J.I.Thorpe et al. Micrometeoroid Events in LISA Pathfinder. The Astrophysical Journal, vol. 883, no. 1, 2019. DOI: 10.3847/1538-4357/ab3649.

[3] P. F. Gath et al., Drag free and attitude control system design for the LISA science mode, in Proceedings of the AIAA Guidance, Navigation and Control Conf. and Exhib., Hilton Head SC, 20-23 August 2007, AIAA 2007 No. 6731 (American Institute of Aeronautics and Astronautics, 2007), DOI: 10.2514/6.2007-6731

[4] S.-F.Wu and D. Fertin, Spacecraft drag-free attitude control system design with quantitative feedback theory, Acta Astronautica 62, 668, 2008, DOI:10.1016/j.actaastro.2008.01.038

[5] M. Armano et al., Sub-femto-g free fall for gravitational wave observatories: Lisa pathfinder results, Phys.Rev. Lett. 116(23), 231101(10), 2016, DOI: 10.1103/PhysRevLett.116.231101

[6] J.Wertz, Spacecraft Attitude Determination and Control, 2002, DOI: 10.1007/978-94-009-9907-7

[7] O. Jennrich, LISA technology and instrumentation, Class. QuantumGrav. 26, 153001, 2009, DOI: 10.1088/0264-9381/26/15/153001

[8] J.W. Conklin, Drift mode accelerometry for spaceborne gravity measurements, Journal of Geodesy, 89, pp 1053-1070, 2015, DOI: 10.1088/0264-9381/28/9/094006

[9] Schumaker B. Disturbance reduction requirements for LISA, Classical and Quantum Gravity, 2003, DOI: DOI 10.1088/0264-9381/20/10/327

[10] R. Sánchez Maestro, J. Veenman, J. Cardín, J. Grzymisch, V. Preda, GNC Functional Architecture Design and Implementation of the LISA Drag Free Control System, ESA GNC-ICATT 2023, 2023, DOI: 10.5270/esa-gnc-icatt-2023-119

[11] Brunton, S. L., Nathan Kutz, J., Manohar, K., Aravkin, A. Y., Morgansen, K., Klemisch, J., ... & McDonald, D., Data-driven aerospace engineering: reframing the industry with machine learning. AIAA Journal, 59(8), 2820-2847, 2021, DOI: 10.2514/1.J060131

# Annex I: Coordinate Frames

All reference frames used are right handed: this means Z=cross(X, Y).

**Orbit Inertial Frame [OIF]**

The Orbit Inertial Frame is used to describe the S/C translational dynamics. It is chosen to be coincident with the "mean ecliptic and equinox of J2000", so defined: Ecliptic coordinates based upon J2000 frame, non-rotating with respect to stars, non-accelerating origin.

***Centre:*** Solar System Barycenter (SBB).

***X-axis:*** Intersection of equatorial and ecliptic planes, called vernal equinox.

***Z-axis:*** Orthogonal to the Ecliptic plane.

***Y-axis:*** Completes the right-hand turn.

**Relative Inertial Frame [RIF]**

The Relative Inertial Frame is used to describe the TM translational dynamics relative to the S/C instantaneous CoM.

***Centre:*** Spacecraft instantaneous CoM . Varying with the configuration "k" (TM grabbed/released) and the rotating elements relative orientation (telescopes/antenna).

***X-axis:*** [OIF] *x-axis.*

***Y-axis:*** [OIF] y-*axis.*

***Z-axis:*** [OIF] *z-axis.*

**Earth Hill's Frame [EHF]**

The Earth Hill's frame is used to describe (a-posteriori) the formation translational relative motion with respect to the Earth.

***Centre:*** Earth center.

***X-axis:*** Aligned with the radial direction from the Sun to the Earth.

***Z-axis:*** Aligned with the Earth orbital momentum.

***Y-axis:*** Completes the right-hand turn.

**Formation Hill's Frame [FHF]**

The Formation Hill's frame is used to describe (a-posteriori) the S/C translational relative motion with respect to the formation centroid.

***Centre:*** Formation centroid.

***X-axis:*** Aligned with the radial direction from the Sun to the formation centroid.

***Z-axis:*** Aligned with the formation orbital momentum.

***Y-axis:*** Completes the right-hand turn.

**Geometry Fixed Frame [GFF]**

The Geometry Fixed frame is used as a supporting frame to define the S/C geometry fixed properties.

***Centre****:* Arbitrary point in the S/C, fixed to the S/C geometry.

***X-axis:*** Bisector of the *x-axes* of the MOSA, when they are at their rest position (i.e. in the middle of their dynamic pointing range).

***Z-axis:*** Aligned with the *z-axis* of the MOSA, i.e. aligned with the pivot axes and perpendicular to the formation plane.

***Y-axis:*** Completes the right-hand turn.

**Rigid Body Frame [RBF]**

The Rigid Body Frame is used to define the S/C absolute attitude dynamics.

***Centre****:* Spacecraft instantaneous CoM. Varying with the configuration "k" (TM grabbed/released) and the rotating elements relative orientation (telescopes/antenna).

***X-axis:*** [GFF] *x-axis.*

***Y-axis:*** [GFF] *y-axis.*

***Z-axis:***[GFF] *z-axis.*